Development 135, 159-169 (2008) doi:10.1242/dev.009050

Insertional mutagenesis by the *Tol2* transposon-mediated enhancer trap approach generated mutations in two developmental genes: *tcf7* and *synembryn-like*

Saori Nagayoshi[1], Eriko Hayashi[2], Gembu Abe[1], Naoki Osato[3], Kazuhide Asakawa[1], Akihiro Urasaki[1], Kazuki Horikawa[2,*], Kazuho Ikeo[3,4], Hiroyuki Takeda[2] and Koichi Kawakami[1,4,†]

Gene trap and enhancer trap methods using transposon or retrovirus have been recently described in zebrafish. However, insertional mutants using these methods have not been reported. We report here development of an enhancer trap method by using the *Tol2* transposable element and identification and characterization of insertional mutants. We created 73 fish lines that carried single copy insertions of an enhancer trap construct, which contained the zebrafish *hsp70* promoter and the GFP gene, in their genome and expressed GFP in specific cells, tissues and organs, indicating that the *hsp70* promoter is highly capable of responding to chromosomal enhancers. First, we analyzed genomic DNA surrounding these insertions. Fifty-one of them were mapped onto the current version of the genomic sequence and 43% (22/51) were located within transcribed regions, either exons or introns. Then, we crossed heterozygous fish carrying the same insertions and identified two insertions that caused recessive mutant phenotypes. One disrupted the *tcf7* gene, which encodes a transcription factor of the Tcf/Lef family mediating Wnt signaling, and caused shorter and wavy median fin folds and pectoral fins. We knocked down Lef1, another member of the Tcf/Lef family also expressed in the fin bud, in the *tcf7* mutant, and revealed functional redundancy of these factors and their essential role in establishment of the apical ectodermal ridge (AER). The other disrupted the *synembryn-like* gene (*synbl*), a homolog of the *C. elegans synembryn* gene, and caused embryonic lethality and small pigment spots. The pigment phenotype was rescued by application of forskolin, an activator of adenylyl cyclase, suggesting that the *synbl* gene activates the $G\alpha_s$ pathway leading to activation of adenylyl cyclase. We thus demonstrated that the transposon-mediated enhancer trap approach can indeed create insertional mutations in developmental genes. Our present study provides a basis for the development of efficient transposon-mediated insertional mutagenesis in a vertebrate.

KEY WORDS: Zebrafish, *tcf7*, *synembryn*, Enhancer trapping, Insertional mutagenesis

INTRODUCTION

In zebrafish, phenotype-driven mutagenesis screens have been performed by two ways. First, chemical mutagenesis screens using ENU have identified hundreds of mutations that cause defects in various processes of embryonic development (Driever et al., 1996; Haffter et al., 1996). Identification of genes responsible for the mutant phenotypes requires positional cloning, which is still laborious (although sequencing and annotation of the genome are nearing completion). Second, a pseudotyped retrovirus has been used to mutagenize the genome (Gaiano et al., 1996). By using this approach, more than 300 recessive lethal mutants and the mutated genes have been identified (Amsterdam et al., 2004). However, a large-scale insertional mutagenesis screen using pseudotyped retrovirus is demanding in terms of labor and space because it requires raising of a large number of F2 families to identify mutant phenotypes in F3 embryos (Amsterdam et al., 1999).

Recently, gene trap and enhancer trap methods were developed in zebrafish. In gene trapping, a *Tol2* transposon construct containing a splice acceptor and the GFP gene was constructed. When the construct was integrated within a gene and the splice acceptor trapped its transcript, GFP is expressed (Kawakami et al., 2004). In enhancer trapping, a *Sleeping Beauty* construct containing a modified EF1α promoter and the GFP gene (Balciunas et al., 2004), a *Tol2* construct containing the *keratin8* promoter and the GFP gene (Parinov et al., 2004), and a retroviral construct containing the *gata2* promoter and the YFP gene (Ellingsen et al., 2005) were used. When the enhancer trap constructs were integrated in the genome and the minimal promoters were activated by enhancers, GFP or YFP is expressed in regulated fashions. It has been demonstrated that these methods can create transgenic fish expressing the reporter proteins in specific cells, tissues and organs, which are useful resources for developmental biology. However, it has not been reported that insertions of these gene trap or enhancer trap constructs can cause any observable mutant phenotype.

We found that the medaka fish *Tol2* element encodes a fully functional transposase (Kawakami et al., 1998; Kawakami and Shima, 1999; Kawakami et al., 2000) and, since then, have been developing genetic methods in zebrafish by using *Tol2* (Kawakami, 2005). Our goal is to develop an efficient transposon-mediated insertional mutagenesis method as follows. First, random integrations of a gene trap or an enhancer trap construct are created in the genome of the germ cells in the fish (F0) injected with a transposon-donor plasmid and the transposase mRNA. Second, F1 embryos exhibiting unique GFP expression patterns are collected and raised. Third, by mating male and female F1 fish that carry the

[1]Division of Molecular and Developmental Biology, National Institute of Genetics, Mishima, Shizuoka 411-8540, Japan. [2]Department of Biological Sciences, University of Tokyo, Tokyo 113-0033, Japan. [3]Center for Information Biology and DNA Data Bank of Japan, National Institute of Genetics, Mishima, Shizuoka 411-8540, Japan. [4]Department of Genetics, The Graduate University of Advanced Studies (SOKENDAI), Mishima, Shizuoka 411-8540, Japan.

*Present address: Research Institute for Electronic Science, Hokkaido University, Sapporo 060-0812, Japan
†Author for correspondence (e-mail: kokawaka@lab.nig.ac.jp)

Accepted 19 October 2007

same insertion, F2 embryos are analyzed for the mutant phenotype. If an insertion disrupted an essential gene, homozygous embryos show a mutant phenotype. Finally, the gene responsible for the mutant phenotype can be cloned rapidly, as the locus is tagged by the transposon. Zebrafish researchers should benefit from this methodology because it will require maintenance of smaller numbers of F1 fish than chemical mutagenesis or retroviral mutagenesis, and the F2 screen will be carried out within a shorter period of time than the F3 screen.

As a first step toward this goal, it is important to demonstrate that a transposon-mediated gene trap or enhancer trap method can indeed create a mutant. In our previous gene trap screen, we created homozygous embryos by mating, but could not identify recessive phenotypes (Kawakami et al., 2004; Kotani et al., 2006). In addition, in the previous gene trap and enhancer trap screens using transposons and retrovirus, recessive mutant phenotypes have not been analyzed extensively (Balciunas et al., 2004; Ellingsen et al., 2005; Parinov et al., 2004). In the present study, we constructed an enhancer trap construct containing the zebrafish *hsp70* promoter and the GFP gene, performed an enhancer trap screen, and established fish lines expressing GFP in specific cells and tissues. We then analyzed phenotypes of homozygous embryos by crossing these lines and found that insertions in the *tcf7* and the *synembryn-like* (*synbl*) gene caused recessive mutant phenotypes. Tcf7 is a transcription factor mediating Wnt signaling. Although the zebrafish *tcf7* gene was cloned previously (Veien et al., 2005), no mutation has been reported. *synbl* is a zebrafish homolog of the *C. elegans synembryn* gene, the product of which has been shown to activate both the $G\alpha_q$ and $G\alpha_S$ pathway, leading to production of diacylglycerol and cyclic AMP, respectively (Miller et al., 2000; Schade et al., 2005). Previously, a mutation of *synbl* was identified by retroviral insertional mutagenesis (Amsterdam et al., 2004), but its phenotype has not been characterized in detail. We will describe characterization of these mutants and demonstrate that insertions of the enhancer trap construct can indeed disrupt the function of developmental genes.

MATERIALS AND METHODS

Construction of T2KHG transgenic fish

T2KHG contains the *hsp70* promoter (a kind gift from Dr J. Kuwada) (Halloran et al., 2000), the GFP gene and the polyA signal between *Tol2* cis-sequences (Urasaki et al., 2006) (see Fig. 3A). A DNA/RNA mixture (1 nl) containing 30 ng/μl plasmid DNA harboring T2KHG and 5 ng/μl transposase mRNA synthesized in vitro was injected into fertilized eggs. F1 fish were analyzed under a fluorescent microscope MZ 16 FA (Leica).

Computational analyses

The integration sites were mapped on the zebrafish genome sequence (Zv6) by BLAT (Kent, 2002). Fifty-one random insertions were created 10,000 times by using the computer system in DDBJ, NIG. The locations of mRNA and Ensemble transcripts were obtained from all_mrna.txt.gz and ensGene.txt.gz (http://hgdownload.cse.ucsc.edu/goldenPath/danRer4/database/), and analyzed by using in-house Perl scripts. RIC8A and RIC8B were aligned by CLUSTAL W (Thompson et al., 1994), and the phylogenetic tree was constructed by the neighbor-joining method (Saitou and Nei, 1987) and the minimum evolution method (Rzhetsky and Nei, 1992) with p-distance. Each node of the phylogenetic tree was evaluated by 1000 bootstrap replications (Felsenstein, 1985).

Whole-mount in situ hybridization

Probes were synthesized with DIG RNA labeling kit (Roche), and purified with mini Quick Spin RNA Columns (Roche). Prehybridization and hybridization were performed at 65°C for 1 hour to over night. The samples were washed in 66% formamide/2×SSCT at 65°C for 30 minutes, in 33% formamide/2×SSCT at 65°C for 30 minutes, in 2×SSCT at 65°C for 15 minutes, and in 0.2×SSCT at 65°C for 30 minutes twice. The samples were then incubated in blocking solution (150 mM maleic acid, 100 mM NaCl, 5% blocking reagent (Roche), 5% new born calf serum, pH 7.5, 0.1% Tween-20) at 4°C overnight, then incubated with 1/4000-1/8000 volume of anti-digoxigenin-AP Fab-fragments (Roche) at room temperature for 4 hours or at 4°C overnight. Samples were washed in maleic acid buffer (150 mM maleic acid, 100 mM NaCl, 0.1% Tween-20, pH 7.5) at room temperatures for 25 minutes three times and then overnight. The signals were detected by using BCIP/NBT Color Development Substrate (Promega). The reaction was stopped by washing with PBS.

Southern blot hybridization and PCR analyses

Southern blot hybridization, inverse PCR, linker-mediated PCR, RT-PCR, 3′ RACE and 5′ RACE were carried out as described previously (Kawakami, 2004; Kotani et al., 2006). Primers used for these analyses are as follows.

HG2A: 5′-GAG GAG AAG AAG GGC CAT CTC ATT C-3′ (forward) and 5′-CTA CAT AAC ACT CTC GAA AAT GAT C-3′ (reverse)

HG3A: 5′-GTC CTG AAC TCA ATC TGT CAT C-3′ (forward) and 5′-CTG AGT TAC CTG AGA ACT GTG A-3′ (reverse)

HG6A: 5′-TCC AGC ACT GAA GTA TGC AGA AAT G-3′ (forward) and 5′-TCA CAG TTT GGC AGC CAT GAA G-3′ (reverse)

HG6B: 5′-ATG TCT TCC AAG CAA GCC ACC TC-3′ (forward) and 5′-GTG TCA TTC TCA CTG CTG TAG TCC-3′ (reverse)

HG6C: 5′-AGT CGG TTT TAT GTT GTC GGA AAA G-3′ (forward) and 5′-TCT GTA GGA TGA GTA GAG CGA-3′ (reverse)

HG6D: 5′-AGC CGT GAG TCT GTT CAG CTG C-3′ (forward) and 5′-CCT TGC CAT CAC AGA TGC CGT T-3′ (reverse)

HG10A: 5′-CAG CGA TTG ACT GTT TTC CGC AAC-3′ (forward) and 5′-CTA CTC TGA ATG AAC AGA CTG TTG-3′ (reverse)

HG21A: 5′-GCA GAT TGA ACT CAT CAC CAC TGC-3′ (forward) and 5′-CAC TGA TCA GGC TTT TAT GCG AGT-3′ (reverse)

HG21B: 5′-CAG TGT GAT CCC ACG AGC TCC TCC-3′ (forward) and 5′-CTT CAG ATC TTC TAG TCC AGT AGA-3′ (reverse)

HG21C: 5′-GAC GTC TTG AGA AAG TTT GGA T-3′ (tcf7-f1) and 5′-GGT TTG TCA GGT GAT AGA CAG G-3′ (reverse)

HGn8H: 5′-GTG CAG AAG GAC TGA CAG TGT T-3′ (synbl-f) and 5′-CTC GAC GGC AGC TCA TTC TTC T-3′ (synbl-r2)

HGn43A: 5′-GTT TGA CCT GGT GCA TTA CGA G-3′ (forward) and 5′-TCA AGG GCT TTT CTG CTG GAG T-3′ (reverse)

ric8a: 5′-GGA ACA GCG ATG AAA ATG GAC T-3′ (forward) and 5′-GTG GGT TAA ATT AAG TCG AAC C-3′ (reverse)

To prepare RNA from heat-shocked embryos, about ten 24 hpf embryos are placed at 40°C for 15 minutes in a microtube, and lysed in TRIzol reagent (Invitrogen) immediately after the heat-shock treatment.

MO injection

Antisense morpholino oligonucleotides (MO) (Gene Tools) against translation initiation sites of *tcf7* (*tcf7*-MO) and *lef1* (*lef1*-MO) and a splice donor of *synbl* (*synbl*-MO) were synthesized:

tcf7-f2: 5′-GTG TTT CCA AAC ATG TAT GAG T-3′
tcf7-r2: 5′-GAC TGT TTG TTA GTT TGA GGC T-3′
tcf7-f3: 5′-GAA CGA CGA GAT GAT CGC GTT T-3′
synbl-r: 5′-CTA CGA TCA CAA GGC AAA TAC C-3′
Tol2-OUT: 5′-AGG ACC AAT GAA CAT GTC TGA CCA A-3′
tcf7-r3: 5′-GGG ACT GGG GTT GAA GTG TTC A-3′
tcf7-MO: GCT GCG GCA TGA TCC AAA CTT TCT C
symbl-MO: ACT GTC ACT CTC ACC TTA TCA CAG G
lef1-MO: CTC CAC CTG ACA ACT GCG GCA TTT C

One-cell stage embryos were injected with 0.1-1 nl of 1-3 mg/ml MOs suspended in H_2O using FemtoJet (Eppendorf).

Pigmentation analysis and forskolin treatment

Embryos were placed in the dark for at least 30 minutes and then observed soon after they were transferred onto the stage of a microscope. One-cell stage embryos were soaked in 1 μM or 2 μM of forskolin (Calbiochem) dissolved in 1% DMSO. As a control, embryos were soaked in 1% DMSO.

RESULTS

An enhancer trap screen using the *Tol2* enhancer trap construct

We constructed T2KHG that contained the zebrafish *hsp70* promoter and the EGFP gene (see Fig. 3A). We expected that transcription from the *hsp70* promoter to be activated at normal temperatures when it was influenced by chromosomal enhancers. We co-injected transposon-donor plasmid DNA containing the T2KHG construct and the transposase mRNA, crossed 77 injected fish with wild-type fish, and analyzed at least 40 embryos from each cross for GFP expression. We found that offspring (F1) from 70% (54/77) of the injected fish carried T2KHG insertions and showed more than 100 different GFP expression patterns. The GFP-positive F1 fish were raised and analyzed by Southern blot hybridization. The number of transposon insertions carried by individual F1 fish varied, from one to more than ten. Excluding fish with more than ten insertions, we analyzed 276 F1 fish and detected 215 different transposon insertions. These fish were further outcrossed to establish fish lines with single insertions. In the course of the outcross, we observed a total of 125 unique GFP expression patterns (Table 1).

Cloning and identification of integration sites

In order to clarify relationship between the expression pattern and the insertion, we established 73 transgenic fish lines that carried single copy insertions of T2KHG (Table 1, Fig. 1) (see Table S1 in the supplementary material). This confirmed that these expression patterns were indeed caused by single T2KHG insertions. We treated some of these lines by heat shock and observed strong GFP expression throughout the body, indicating that the *hsp70* promoters on T2KHG integrated in various loci were still capable of responding to heat shock (data not shown). Although these fish lines expressed GFP in temporally and spatially restricted fashions, most of them expressed GFP weakly in the heart at 24 hpf, and in the heart, skeletal muscle and lens at day 5. We performed whole-mount in situ hybridization and found that the *hsp70* mRNA was detected in the same regions at normal temperatures (data not shown), indicating that these reflected the basal activity of the *hsp70* promoter. We also noticed that the *hsp70* promoter showed maternal expression.

We cloned and sequenced genomic DNA surrounding the 73 insertions. Fifty-one insertions were successfully mapped by BLAT against the zebrafish genome (Zv6) (see Table S1 in the supplementary material). First, these sequences were subjected to a computational analysis to determine whether the insertions were located within transcribed regions. Thirty-three percent of them (17/51) were localized within transcribed regions defined based on mRNA (all_mrna.txt.gz) and Ensembl (ensGene.txt.gz) transcripts. It was estimated by a computational analysis that, if transposon hit the zebrafish genome at random, 37.5% of the insertions would be located within the transcribed regions, indicating that the observed and the estimated frequencies are not statistically different. By comparison, we performed a similar computational analysis on previously reported 92 integration sites created by a retroviral enhancer trap construct (Ellingsen et al., 2005). Fifty one of them were mapped on the genome and 23.5% (12/51) were located within the transcribed region. With statistical significance, this frequency is lower than that observed in our present screen ($P<0.05$). The frequency calculated for the retroviral enhancer trapping is lower than the previous estimate (41%) (Ellingsen et al., 2005) as we used more stringent criteria for transcribed regions here.

Table 1. Summary of the enhancer trap screen

Injected fish mated	77
Founder fish identified	54
Number of insertions detected	215
GFP patterns identified	>125
Integration site cloned	73
Integration sites mapped on the genome	51
Insertions located within transcribed regions	22
Homozygous embryos analyzed	54
Recessive mutants identified	2

Expression patterns of genes at the integration sites

To compare the GFP expression patterns with expression patterns of the genes at the integration sites, we performed RT-PCR for eight genes identified in HG3A, HG6C, HG6D, HG10A, HG10B HG21C, HGn8H and HGn43A. In all of these cases, cDNA clones were successfully obtained, indicating that the genes were indeed transcribed. Furthermore, we performed RT-PCR for eight genes found at the integration sites in HG2A, HG6A, HG6B, HG21A, HG21B, HG21K, HGn15B and HGn54A, which are predicted genes based on either EST, GenScan or Nscan, but not are the mRNA or Ensembl transcripts. In five cases (HG2A, HG6A, HG6B, HG21A, and HG21B), RT-PCR products were amplified, indicating that these were transcribed. Taking these into account, 43% (22/51) of the insertions were localized within protein-coding transcribed genes (Table 1) (see Table S1 in the supplementary material).

Then, we performed whole-mount in situ hybridization using the *chot1* (HG2A), *cyp2e2* (HG3A), *ide* (HG6A), *soxlz* (HG6B), *uros* (HG6C), *asb1* (HG6D), *ripk2* (HG10B), *lmo7* (HG21A), *hg21b* (novel gene; HG21B), *tcf7* (HG21C) and *synbl* (HGn8H) probes. Expression of *chot1* (myotome; Fig. 2A,B), *cyp2e2* (yolk; Fig. 2C,D), *ide* (myotome, Fig. 2E,F), *soxlz* (myotome; Fig. 2G,H), *uros* (ventral mesoderm; Fig. 2I,J), *lmo7* (myotome; Fig. 2K,L), *hg21b* (otic vesicle; Fig. 2M,N),and *tcf7* (median fin fold; Fig. 3B,C) recapitulated respective GFP expression patterns, at least partly, indicating that the *hsp70* promoter was activated by enhancers that regulated those genes. By contrast, *asb1* (HG6D), *synbl* (HGn8H) and *ripk2* (HG10B) were expressed weakly in the whole body (data not shown). These were not similar to the GFP expression patterns. In these cases, the *hsp70* promoter was likely to be influenced by enhancers that regulate expression of their neighboring genes. We will describe such an example in the case of HGn8H below.

The HG21C insertion disrupted the *tcf7* gene

To elucidate whether the T2KHG insertions can cause observable mutant phenotypes, we analyzed phenotypes of homozygous embryos for 54 insertions including 20 insertions mapped within transcribed regions (see Table S1 in the supplementary material). We found morphological defects in the progeny from HG21C and HGn8H heterozygous parents.

In HG21C, T2KHG was integrated within the *tcf7* gene that encodes a transcription factor downstream of Wnt signaling (Fig. 3A, Fig. 5A). GFP fluorescence and *gfp* mRNA were detected in the dorsal retina, diencephalon, tail bud and median fin fold at 24 hpf (Fig. 1, Fig. 3B). Although *tcf7* mRNA was detected in broad areas in the brain, *gfp* mRNA did not show such an expression pattern (Fig. 3B,C), suggesting that a putative brain enhancer of *tcf7* did not influence the *hsp70* promoter. We analyzed 568 embryos obtained from HG21C heterozygous parents (Fig. 3D-H). One hundred and fifty-four out of 420 GFP-positives, but none of 148 GFP-negatives, showed short and wavy median fin folds at 60-72 hpf. Then, we performed genotyping by PCR and found that all of 83 GFP-positives with the fin phenotype were homozygous and all of 139 GFP-positives without the fin phenotype were heterozygous (Fig.

3I,J). These results strongly suggested that the observed fin defect is a recessive mutant phenotype caused by the transposon insertion. The length of the median fins was restored to nearly the wild-type level after day 6, but the wavy edge was observed at least until day 14 (data not shown). The homozygous fish were viable and fertile.

In wild-type embryos, *tcf7* expression in the median fin fold was detectable after the 15-somite stage, was maintained through 24 hpf, then was gradually weakened at 36 hpf, and almost disappeared by 48 hpf (Fig. 3K,M). *tcf7* is also expressed in the pectoral fin bud, strongly in the apical ectodermal ridge (AER) and weakly in the

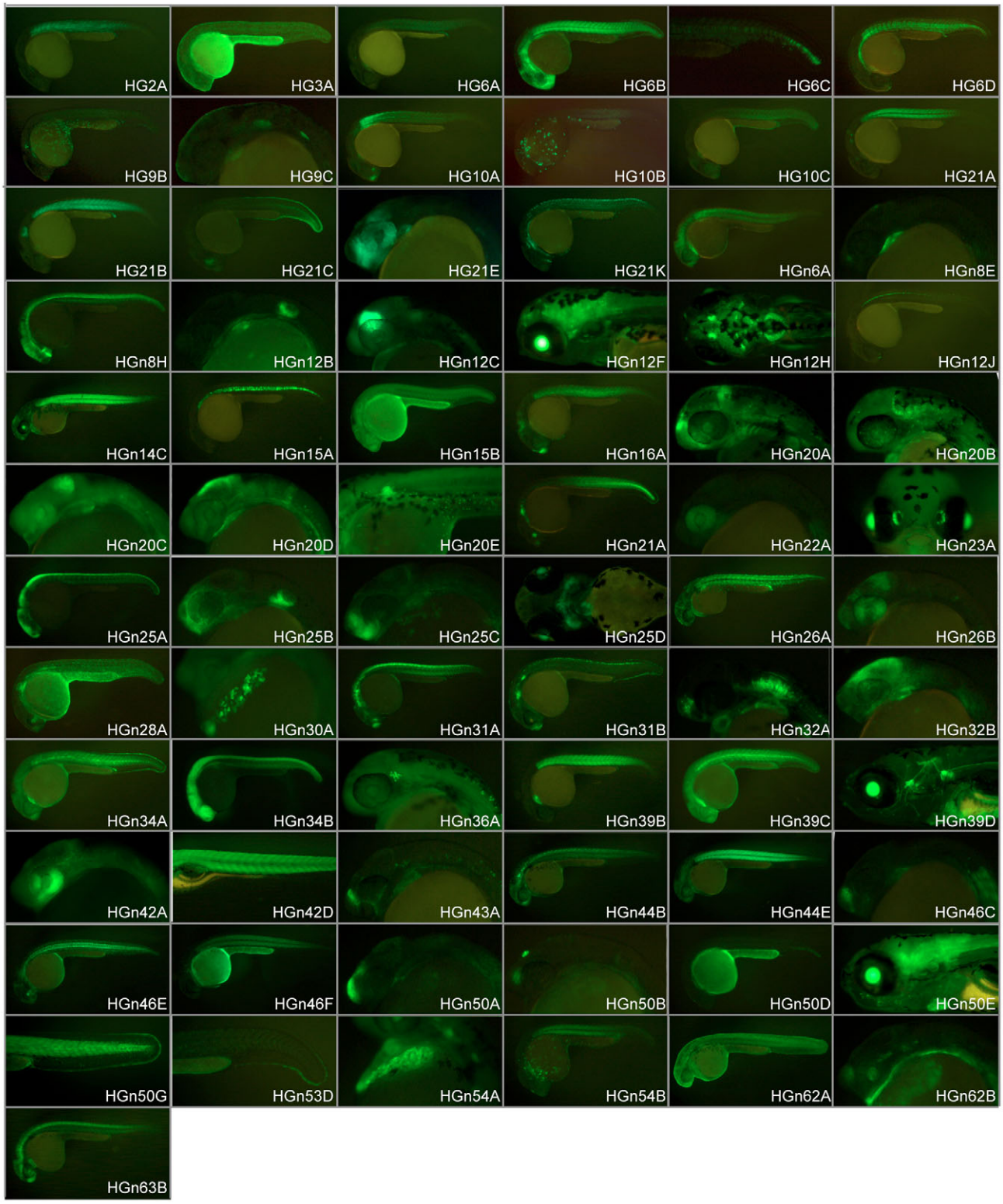

Fig. 1. GFP expression patterns in enhancer trap lines. GFP expression patterns in 24 hpf to day 5 embryos carrying single T2KHG insertions. Numbers after HG represent individual founder fish. Letters after numbers represent distinct patterns obtained from single founder fish. The patterns and transposon integration sites are described in Table S1 in the supplementary material.

mesenchyme at 36-48 hpf (Fig. 3O,Q). In HG21C homozygous embryos, the *tcf7* expression was not detected in these fins and the other regions (Fig. 3L,N,P,R; data not shown). We observed the pectoral fins in the homozygous embryos carefully and found that the fins were smaller and showed wavy edges at 60-72 hpf (Fig. 3S,T). To confirm that the observed defects in fin development were indeed caused by a decreased Tcf7 activity, we injected *tcf7*-MO into one-cell stage embryos. In this experiment, the HG21C heterozygous embryos were used as it is easier to observe fin morphology because of GFP fluorescence. Fifty-nine percent and 84% of embryos injected with 0.1 ng and 0.3 ng *tcf7*-MO, respectively, exhibited shorter and wavy pectoral fins and median fin folds, which resembled the phenotype observed in the homozygous embryos (Fig. 3U-W).

Roles of Tcf7 and Lef1 in outgrowth of the pectoral fin

tcf7 and *lef1*, both members of the Lef/Tcf family of transcription factors that mediate Wnt signaling, are expressed in the fin bud and are thought to be functionally redundant (Veien et al., 2005). However, this notion has not yet been tested. Taking advantage of the *tcf7* mutant, we injected *lef1*-MO into HG21C homozygous and heterozygous embryos to examine their possible functional redundancy in pectoral fin development. Fin outgrowth was severely reduced in 79% (45/57) of MO-injected homozygous embryos but not in MO-injected heterozygous embryos (0/74) (Fig. 4A-C), indicating that Lef1 compensated the loss of the Tcf7 activity and Tcf7 or Lef1 is required for fin outgrowth.

We then analyzed expression of *tcf7* and *lef1* in the pectoral fin bud at the AER induction (28 hpf) and maintenance (38 hpf) stages. The *tcf7* expression was detected strongly in the AER and weakly in the mesenchyme at 28 hpf and 36 hpf (Fig. 4D,F), while the *lef1* expression was detected both in the AER and mesenchyme at 28 hpf and only in the mesenchyme at 36 hpf (Fig. 4E,G). The unique expression of *tcf7* in the AER at 36 hpf may account for the small and wavy fin phenotype observed in the HG21C homozygous embryos at later stages (Fig. 3S,T). To define the defects in *lef1* and *tcf7* loss-of-function embryos, we analyzed expression of mesenchymal (*fgf10*) and ectodermal (*dlx2a*, *fgf24*, *wnt3l* and *fgf8*) markers (Akimenko et al., 1994; Fischer et al., 2003; Norton et al., 2005; Reifers et al., 1998) in the *lef1*-MO-injected embryos. At 28 hpf, the mesenchymal *fgf10* expression was similar in *lef1*-MO-injected wild-type and *tcf7* mutant embryos (Fig. 4H,I). By contrast, expression of *dlx2a* in the AER was severely reduced in the *lef1*-MO-injected *tcf7* mutant embryos; i.e. the expression was absent in about half of the injected embryos and detectable but very weak in the rest (n=11, Fig. 4J,K), suggesting that AER induction was impaired in the *lef1* and *tcf7* loss-of-function embryos. At 38 hpf (48 hpf for *fgf8*), *fgf10* was expressed normally in both *lef1*-MO-injected wild-type and *tcf7* mutant embryos (Fig. 4L,M), while expression of the AER markers *dlx2a*, *fgf24*, *wnt3l* and *fgf8* was absent from the ectoderm in the MO-injected *tcf7* mutants (n=6 each, Fig. 4L-U). The results obtained when wild-type or heterozygous embryos were used for MO injection were essentially indistinguishable (data not shown). From these results, we concluded that Lef7 and Tcf1 are functionally redundant during pectoral fin out growth and play essential role(s) both in the AER induction and maintenance stages.

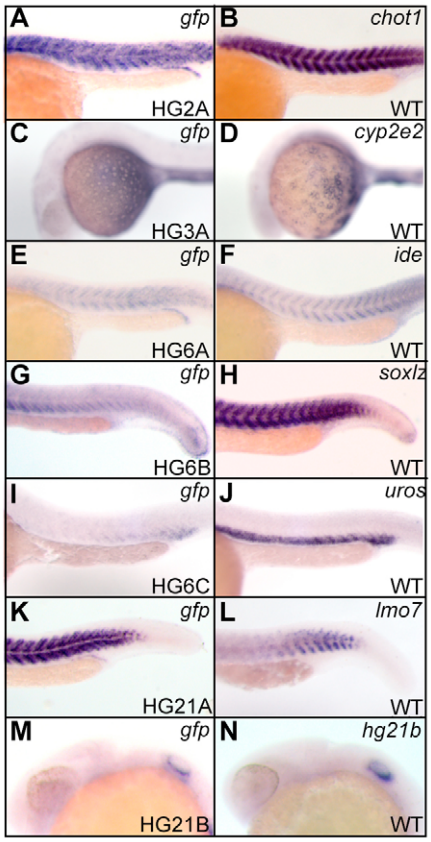

Fig. 2. Expression patterns of genes at the integration sites. (**A**,**C**,**E**,**G**,**I**,**K**,**M**) Whole-mount in situ hybridization of embryos heterozygous for respective insertions (bottom right) at 24 hpf using the *gfp* probe. (**B**,**D**,**F**,**H**,**J**,**L**,**N**) Whole-mount in situ hybridization of wild-type embryos at 24 hpf using probes indicated (top right). Signals were detected in myotome (A,B), yolk (C,D), myotome (E-H), ventral mesoderm (I,J), myotome (K,L) and otic vesicle (M,N).

Characterization of transcripts in the HG21C enhancer trap line

In HG21C, T2KHG was integrated in the coding region in the first exon of the *tcf7* gene (Fig. 5A). To understand how the *tcf7* gene was disrupted, we performed 3′ RACE using nested primers in the first exon. In the HG21C allele, the 3′ RACE products were stopped within the insertion (Fig. 5B). The longest transcript had a capacity to produce a truncated protein of 44 amino acids containing the N-terminal region of Tcf7, which is unlikely to be functional. Then, we performed RT-PCR using the f3 and r3 primers to detect possible transcripts that passed over the insertion. Two faint bands that were detected in HG21C homozygous embryos were cloned and sequenced. These bands represented abnormally spliced transcripts containing premature stop codons (Fig. 5C). As a transcript containing a wild-type sequence of the first exon could not be detected, the HG21C allele is likely to be null.

Furthermore, we analyzed how the *hsp70* promoter is activated in the enhancer trap lines by 5′ RACE. Although the zebrafish *hsp70* promoter has been a useful tool (Halloran et al., 2000; Uemura et al., 2005), the transcription start site has not yet been characterized. First, we prepared RNA from heat-shocked HG21C homozygous embryos, and obtained four 5′ RACE clones. Three of them contained the same A at the 5′ ends, which we designated as position +1, and the other contained A at –2 at the 5′ end (Fig. 5D). Second, we prepared RNA from HG21C homozygous embryos at normal temperatures, and sequenced two 5′ RACE clones. These contained A at +1 and +2 at their 5′ ends (Fig. 5D). Thus, the transcription start sites were nearly the same in both heat-shocked and non heat-

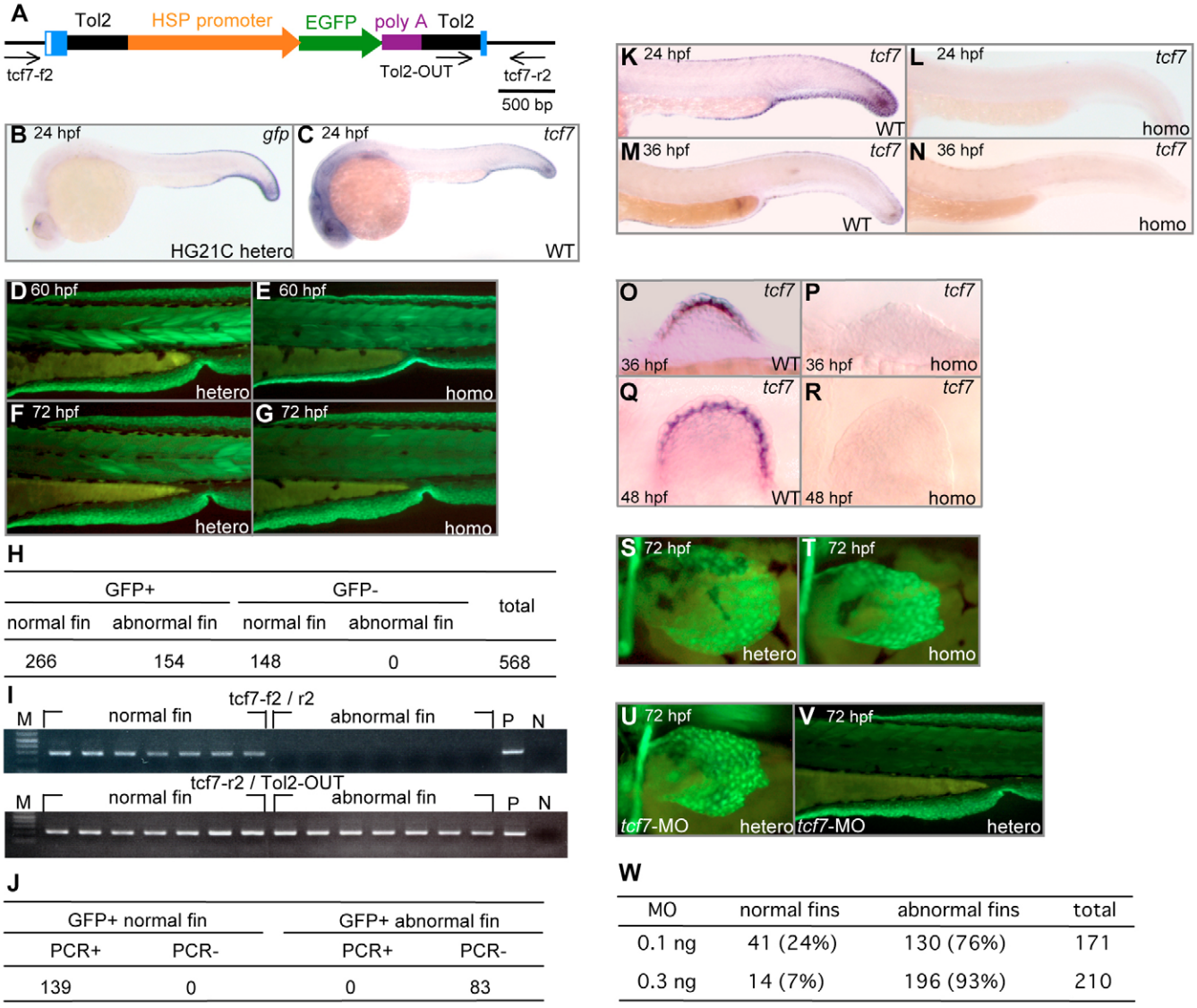

H

GFP+		GFP-		total
normal fin	abnormal fin	normal fin	abnormal fin	
266	154	148	0	568

I

J

GFP+ normal fin		GFP+ abnormal fin	
PCR+	PCR-	PCR+	PCR-
139	0	0	83

W

MO	normal fins	abnormal fins	total
0.1 ng	41 (24%)	130 (76%)	171
0.3 ng	14 (7%)	196 (93%)	210

Fig. 3. The HG21C insertion disrupted the *tcf7* gene. (**A**) The structure of the T2KHG insertion in the *tcf7* gene. T2KHG is composed of *Tol2* sequences (black), the zebrafish *hsp70* promoter (orange), the GFP gene (green) and the SV40 polyA signal (purple). Exons (blue boxes) and 5′ UTR (white box) of the *tcf7* gene are shown. Black arrows indicate positions and directions of primers. (**B**) Whole-mount in situ hybridization of an HG21C heterozygous embryo at 24 hpf using the *gfp* probe. (**C**) Whole-mount in situ hybridization of a wild-type embryo at 24 hpf using the *tcf7* probe. (**D-G**) The median fin fold of HG21C embryos. Heterozygous (D,F) and homozygous (E,G) embryos at 60 hpf (D,E) and 72 hpf (F,G). (**H**) Summary of the linkage between the fin phenotype and the GFP expression. (**I**) Examples of the genotype analysis by PCR using tcf7-f2 and tcf7-r2 (top) and control PCR using tcf7-r2 and Tol2-OUT (bottom). M, DNA size marker; N, no DNA; P, positive control. (**J**) Summary of the genotype analysis. (**K-R**) Whole-mount in situ hybridization using the *tcf7* probe. Wild-type embryos at 24 hpf (K) and 36 hpf (M), and HG21C homozygous embryos at 24 hpf (L) and 36 hpf (N). The pectoral fin buds of wild-type embryos at 36 hpf (O) and 48 hpf (Q), and HG21C homozygous embryos at 36 hpf (P) and 48 hpf (R). (**S**,**T**) The pectoral fins of 72 hpf heterozygous (S) and homozygous (T) HG21C embryos. (**U**,**V**) Microinjection of *tcf7*-MO. The pectoral fin (U) and the median fin (V) of MO-injected HG21 heterozygous embryos at 72 hpf. (**W**) Summary of the numbers of MO-injected embryos that showed abnormal median fin folds and pectoral fins.

shocked conditions, indicating that the *hsp70* promoter on T2KHG was indeed activated by a putative *tcf7* enhancer in the trap line. The 5′ RACE analysis did not amplify the longest 3′ RACE product probably because the smaller amount of transcripts that started from the *tcf7* promoter. We also analyzed four 5′ RACE clones amplified from the HG2A and HG21B lines at normal temperatures. Similar to the 5′ RACE products from HG21C, three and one clones contained A at +1 and A at +2 as the 5′ ends, respectively. In the course of these analyses, we found an intron in the *hsp70* promoter fragment (Fig. 5D). We investigated EST sequences in the database, and found that the endogenous *hsp70* gene also contains an intron in the 5′ UTR.

The HGn8H insertion disrupted the *synembryn-like* gene

In HGn8H, T2KHG was integrated within the first intron of the *synembryn-like* (*synbl*) gene (Fig. 6A). We analyzed 485 embryos obtained from HGn8H heterozygous parents and found that 140

out of 370 GFP-positives, but none of 115 GFP-negatives, showed small pigment spots at day 2, developed edema at day 5, and were gradually degraded (Fig. 6B-F). Then we performed genotyping by PCR and found that all of 37 GFP-positives with the edema phenotype were homozygous and all of 42 GFP-positives without the edema phenotype were heterozygous (Fig. 6G,H), suggesting that the insertion created a recessive lethal mutation.

To determine how the insertion affected the *synbl* transcript, we performed RT-PCR using the synbl-f and r2 primers. In HGn8H homozygous embryos, the RT-PCR product was not detected (Fig. 6I), indicating that the HGn8H insertion interfered with the *synbl* expression nearly completely. To confirm that the mutant phenotype was caused by a decreased Synbl activity, we injected *synbl*-MO into wild-type embryos at the one-cell stage. Eighty percent (105/131) of the MO-injected embryos exhibited small pigment spots, which were similar to the HGn8H mutant phenotypes (Fig. 6S). All of the injected embryos formed edema and were gradually degraded. From these results, we concluded that the HGn8H mutant phenotype was caused by the decreased Synbl activity. In the case of HGn8H, we could not detect a transcript that stopped within the insertion either by 3′ RACE or RT-PCR (data not shown).

In HGn8H, GFP and *gfp* mRNA was expressed in the anterior ventral diencephalon, midbrain and spinal cord at 24 hpf (Fig. 6J,K). By contrast, the *synbl* mRNA was accumulated weakly throughout the body (Fig. 6L). To explain this discrepancy, we hypothesized that

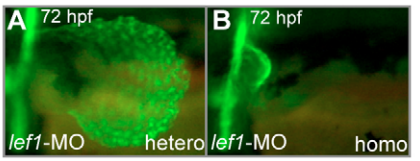

C

genotype	outgrown fin	reduced fin	total
HG21C (-/+)	74	0	74
HG21C (+/+)	12	45	57

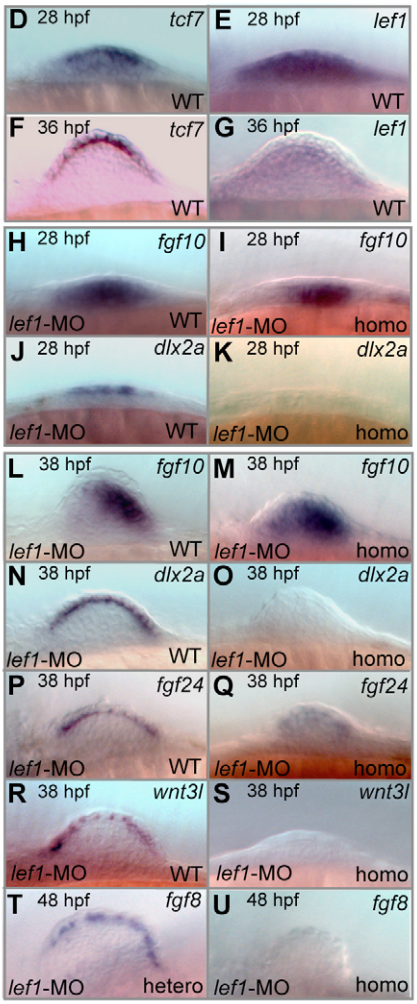

Fig. 4. Roles of Tcf7 and Lef1 in the pectoral fin outgrowth. (**A-C**) Microinjection of *lef1*-MO into HG21C embryos. The pectoral fins of MO-injected heterozygous (A) and homozygous (B) embryos at 72 hpf. (C) Summary of the numbers of MO-injected embryos that showed an outgrown fin or reduced fin phenotype. (**D-U**) The pectoral fins of *lef1*-MO-injected wild-type and HG21C embryos analyzed by whole-mount in situ hybridization. The stages (28 hpf, 36 hpf, 38 hpf and 48 hpf) are shown on the top right. Wild-type (D-H,J,L,N,P,R), heterozygous (T) and homozygous (I,K,M,O,Q,S,U) embryos were used. The probes used are indicated (top right).

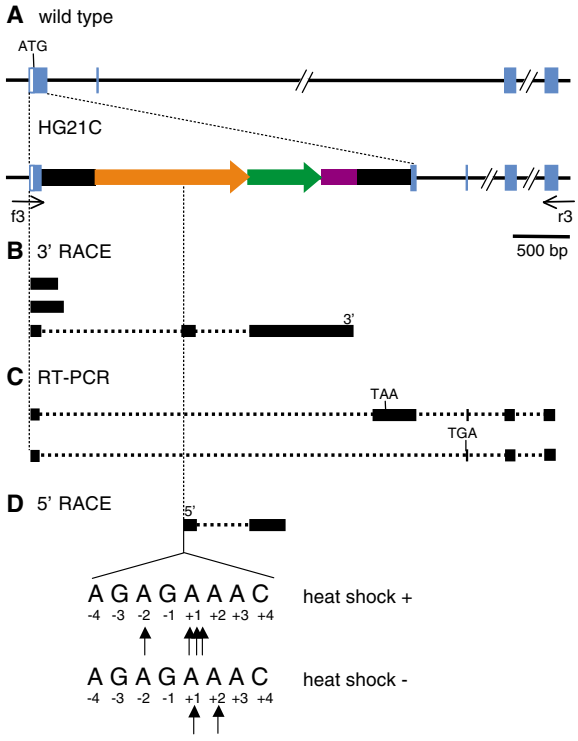

Fig. 5. Transcripts in the HG21C insertion locus. (**A**) The structure of the *tcf7* locus in wild type and the HG21C enhancer trap line. Blue boxes and a white box indicate exons and 5′ UTR, respectively. Positions and directions of primers are shown. (**B**) Three 3′ RACE products (thick lines) identified in homozygous embryos by using nested primers in the first exon. Broken lines indicate regions removed by splicing. (**C**) Two RT-PCR products (thick lines) identified in homozygous embryos using f3 and r3 primers. Broken lines indicate regions removed by splicing. Positions of premature stop codons are shown (TAA and TGA). (**D**) The 5′ RACE products identified in homozygous embryos in heat-shocked and non heat-shocked conditions by using nested primers in the GFP gene. A broken line indicates an intron. Arrows indicate 5′ ends of the 5′ RACE products.

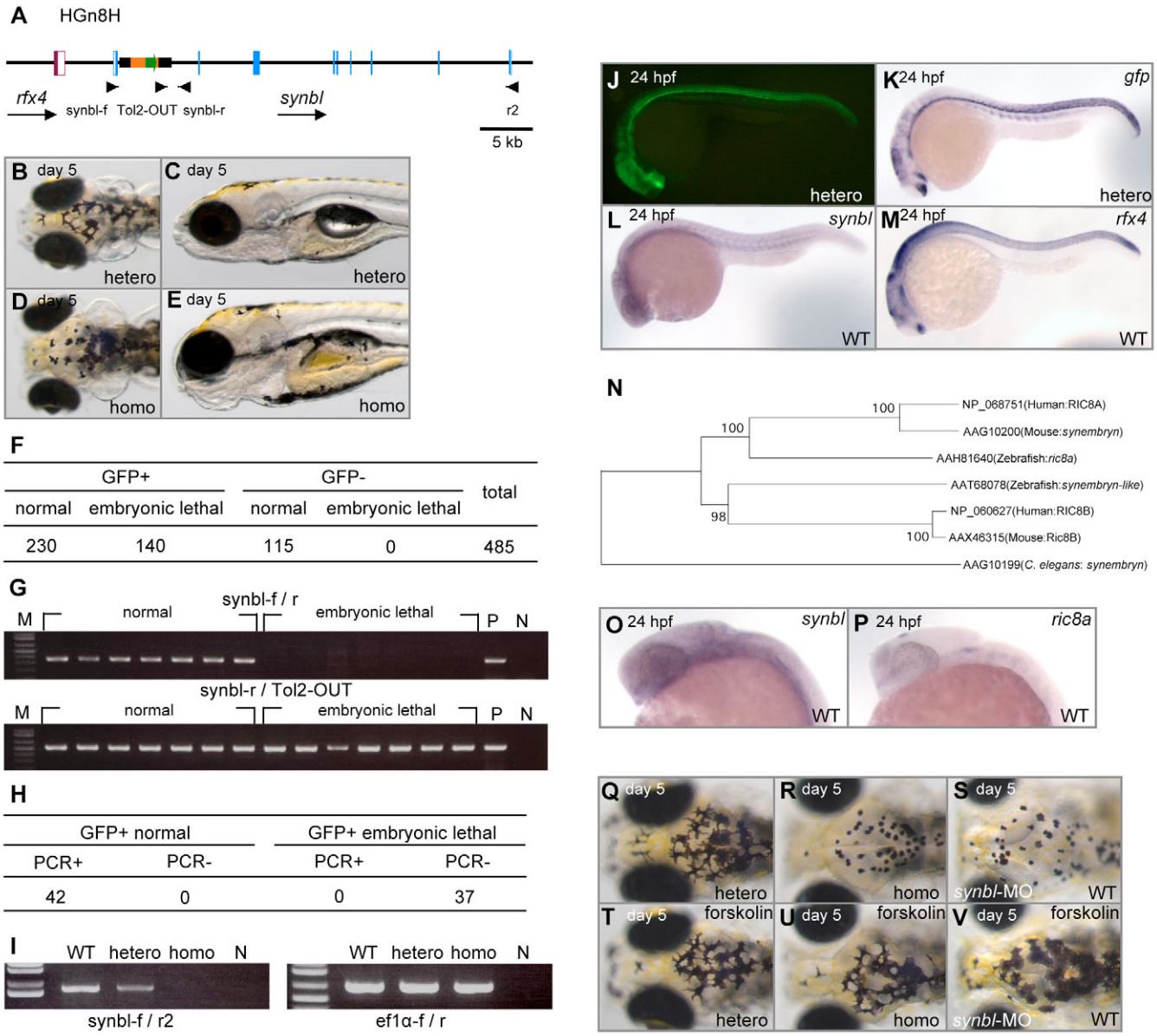

Fig. 6. The HGn8H insertion disrupted the *synembryn-like* gene. (**A**) The structure of the T2KHG insertion in the *synbl* locus in the HG8H enhancer trap line. Arrowheads indicate positions and directions of primers. Blue and purple boxes indicate exons of the *synbl* and *rfx4* genes, respectively. White boxes indicate 5′ and 3′ UTRs. (**B-E**) The pigment and edema phenotype in HGn8H embryos at day 5. Dorsal and side views of heterozygous (B,C) and homozygous (D,E) embryos. (**F**) Summary of the link between embryonic lethality and GFP expression. (**G**) Examples of the genotype analysis by PCR using synbl-f and synbl-r (top) and control PCR using r2 and Tol2-OUT (bottom). M, DNA size marker; N, no DNA; P, positive control. (**H**) Summary of the genotype analysis. (**I**) RT-PCR analysis of wild-type, heterozygous and homozygous embryos using synbl-f and r2 (left). Control RT-PCR using ef1α-f and ef1α-r primers (right). (**J**,**K**) GFP expression pattern in 24 hpf heterozygous embryos. GFP fluorescence (J) and whole-mount in situ hybridization using the *gfp* probe (K). (**L**,**M**) Whole-mount in situ hybridization of 24 hpf wild-type embryos using the *synbl* (L) and *rfx4* (M) probes. (**N**) A phylogenic analysis of vertebrate *synembryn* homologs. (**O**,**P**) Whole-mount in situ hybridization of 24 hpf wild-type embryos using the *synbl* (O) and *ric8a* (P) probes. (**Q-V**) Rescue of the pigment phenotype by forskolin. Pigmentation of heterozygous (Q,T), homozygous (R,U) and *synbl*-MO-injected wild-type (S,V) embryos at day 5. Embryos were soaked in 1 μM (T,U) and 2 μM (V) forskolin.

a putative enhancer that regulates a neighboring gene activated the *hsp70* promoter. To test this hypothesis, we cloned cDNA of the *rfx4* gene that was located ~5 kb upstream of *synbl* (Fig. 6A). *rfx4* encodes a winged helix transcription factor RFX4 which is essential for brain morphogenesis in mice (Blackshear et al., 2003). We found that the *rfx4* mRNA was accumulated in the anterior ventral diencephalons and the spinal cord (Fig. 6M), where the strong *gfp* expression was detected. This result suggested that an *rfx4* enhancer activated the *hsp70* promoter.

Rescue of the *synbl* phenotype by forskolin

In mammals, two *synembryn* homologs, RIC8A and RIC8B, have been identified (Klattenhoff et al., 2003; Tall et al., 2003). The zebrafish genome also contains another *synembryn* homolog (*ric8a*). A phylogenetic analysis showed the zebrafish *synbl* gene is closer to the mammalian RIC8B gene (Fig. 6N). We cloned the zebrafish *ric8a* cDNA (AB354735), analyzed its expression and found that it is expressed rather weakly (Fig. 6O,P). The stronger and broader expression of *synbl* may account for its essential role.

Genetic studies have shown that the *C. elegans synembryn* gene is involved in activation of the $G\alpha_q$ and $G\alpha_S$ pathway, which lead to production of diacylglycerol and cyclic AMP (cAMP), respectively (Miller et al., 2000; Schade et al., 2005). Biochemical studies have shown that rat RIC8A is a GTP exchange factor for Gα proteins (Tall et al., 2003). Therefore, the *synbl* gene may also activate Gα proteins in zebrafish. Recently, it was reported that dispersion of melanosomes is positively regulated by increase in the cellular cAMP level (Logan et al., 2006). These prompted us to hypothesize that the observed small pigment spot is caused by a decrease in the cAMP level. To test this hypothesis, we treated embryos from HGn8H heterozygous parents with forskolin, an activator of the adenylyl cyclase (Seamon et al., 1981). As application of forskolin to zebrafish embryos suppresses the hedgehog pathway and causes gross morphological defects (Barresi et al., 2000), we optimized its concentration. We found 89% (49/55) of homozygous embryos soaked in 1 μM forskolin formed normally dispersed melanosomes (Fig. 6Q,R,T,U), indicating that the pigment phenotype can be rescued by activating adenylyl cyclase. However, the edema and embryonic lethality were not rescued by the forskolin treatment. We then treated *synbl*-MO injected embryos with 2 μM forskolin. Eighty-six percent (118/137) of the treated embryos showed normally dispersed melanosomes (Fig. 6S,V), whereas 88% (57/65) of untreated embryos showed small pigment spots. These results suggested that the small pigment spot in the *synbl* mutant was caused by a decrease in the adenylyl cyclase activity.

DISCUSSION

The efficiency of enhancer trapping using T2KHG

In this study, we identified 125 unique GFP expression patterns from 77 injected fish. This frequency (1.6=125/77) is higher than those reported for other enhancer trap methods; i.e. a *Sleeping Beauty* construct using the modified EF1α promoter (0.03), a *Tol2* construct using the *keratin8* promoter (0.12), a retroviral construct using the *gata2* promoter (0.3) (Balciunas et al., 2004; Ellingsen et al., 2005; Parinov et al., 2004). We think this is due to the highly efficient germline transmission by the *Tol2* transposon system described here (70%), and to the high responsiveness of the *hsp70* promoter to chromosomal enhancers. The responsiveness of a minimal promoter to enhancers can be discussed by comparing frequencies to obtain unique GFP expression patterns per insertions. In this study, 125 GFP expression patterns were identified in 256 F1 fish that harbored a total of 215 insertions. Thus, ~58% (125/215) of T2KHG insertions caused unique GFP expression patterns. By contrast, in the enhancer trap screens using the *keratin8*, modified EF1α and *gata2* promoter, this frequency was estimated as ~28%, ~4% and 14%, respectively (Amsterdam and Becker, 2005; Kawakami, 2005). In *Drosophila*, the *hsp70*, *P*-transposase and *ftz* promoters have been used as minimal promoters for enhancer trap constructs. It was shown that 90%, 20% and 40% of insertions of these constructs caused *lacZ* expression, respectively (Mlodzik and Hiromi, 1992). Thus, both in zebrafish and *Drosophila*, the *hsp70* promoter exhibited the highest enhancer trap activity. A possible disadvantage caused by using the *hsp70* promoter may be its basal transcription activity. We are currently dissecting the zebrafish *hsp70* promoter to remove elements regulating those unwanted basal activities.

Although the *hsp70* promoter was used for an enhancer trap screen reported recently (Scott et al., 2007), its mechanism of action has not been characterized. We demonstrated that the *hsp70* promoter is indeed activated in the enhancer trap lines, strengthening its usefulness as a minimal promoter. In the *Drosophila* and human *hsp70* promoters, short RNA transcripts are produced at the transcription start site in uninduced conditions, and elongation of the paused transcript is stimulated upon heat shock (Brown et al., 1996; Rougvie and Lis, 1988). The zebrafish *hsp70* promoter has not yet been characterized in such a detail. However, the observed common feature, the high responsiveness to enhancers, may suggest that a similar mechanism also operates the zebrafish *hsp70* promoter. It is interesting that, unlike *Drosophila* and human, the zebrafish *hsp70* promoter is TATA-less as there is no TATA sequence upstream of the identified transcription start site. Based on the information about the transcription start site as well as the intron in the 5′ UTR, we aim to construct improved versions of enhancer trap constructs with minimum basal activities.

We found that, in the case of HGn8H, the *hsp70* promoter on T2KHG integrated in the *synbl* gene was probably activated by an enhancer of its neighboring gene: *rfx4*. A similar phenomenon has been described also in retroviral enhancer trapping (Kikuta et al., 2007). How was the *hsp70* promoter affected by an *rfx4* enhancer but not by a *synbl* enhancer? How did the *rfx4* enhancer affect the *hsp70* promoter while not affecting the *synbl* promoter in a wild-type condition? Studies on the *rfx4* and *synbl* enhancers and promoters may illuminate an unknown mechanism that governs specificity between enhancer and promoter.

Roles of Tcf7 and Lef1 in AER formation

We found that Tcf7 and Lef1 are essential for expression of AER markers in the ectoderm in the early and late stages of the pectoral fin development. It has been shown that, in the early limb/fin induction stage, *Wnt2b*, which is expressed in the lateral plate mesoderm (LPM), activates expression of *fgf10* in the mesenchyme of the limb/fin buds in chicken and zebrafish (Kawakami et al., 2001; Ng et al., 2002). In mouse, although *Wnt2b* expression was not detected in LPM, *Fgf10* expression became weaker in $Lef1^{-/-};Tcf7^{-/-}$ embryos and it was suggested that signaling mediated by unidentified Wnt(s) is required to maintain normal levels of *Fgf10* expression (Agarwal et al., 2003). By contrast, our present study indicated that Lef1 and Tcf7 are not required for the mesenchymal *fgf10* expression in zebrafish. Thus, components of Wnt signaling involved in *Fgf10* induction are species specific and additional Tcf genes may compensate the loss of *tcf7* and *lef1* in zebrafish. In addition, our loss-of-function study suggested that the Wnt signaling in the ectoderm mediated by Lef1 and Tcf7 is essential for AER maintenance. This notion is consistent with the previous observations that *Wnt3a*-mediated β-catenin-dependent signaling activates expression of AER markers in the chicken limb ectoderm (Kawakami et al., 2001; Kengaku et al., 1998) and mouse $Lef1^{-/-};Tcf7^{-/-}$ embryos exhibit a defect in limb development (Galceran et al., 1999).

As *tcf7* is exclusively expressed also in the dorsal retina, it can be speculated that Tcf7 may have a unique role also in this area (Fig. 3B,C) (Veien et al., 2005). At present, however, we have not detected any obvious defects in the dorsal retina (M. Yamaguchi, I. Masai, E. S. Veien and R. Dorsky, personal communications). It has been shown that the same factors, such as Dlx genes, *fgf24* and *sp9*, are expressed both in the AER and the edge of the median fin fold (Abe et al., 2007). Although a mechanism that regulates outgrowth of the median fin folds is largely unknown, we noticed that outgrowth of the median fins was also impaired in the *lef1* and *tcf7* loss-of-function embryos (data not shown), suggesting that similar Wnt and Fgf signaling pathways regulate development of both pectoral fins and median fin folds.

The zebrafish *synembryn-like* gene activates the $G\alpha_S$ pathway

It has been shown that *synembryn* and its mammalian homologs are involved in activation of Gα proteins (Klattenhoff et al., 2003; Miller et al., 2000; Schade et al., 2005; Tall et al., 2003). Recently, in zebrafish, it was shown that dispersion of melanosomes is enhanced by activation of adenylyl cyclase (Logan et al., 2006). Our study established a link between these two processes. The disruption of the *synbl* function caused aggregation of melanosomes, which could be restored by activation of adenylyl cyclase. Therefore, it is reasonable to postulate that the *synbl* gene, a homolog of mammalian RIC8B, is involved in activation of the $G\alpha_S$ pathway, leading to activation of adenylyl cyclase and dispersion of melanosomes. The *synbl* gene may be involved in regulation of pigmentation in wild-type conditions, such as a physiological color change during background adaptation. However, the edema phenotype and the embryonic lethality were not rescued by the forskolin treatment. The concentration of forskolin may not be high enough to rescue those phenotypes, or alternatively, those phenotypes may be caused by failures in activation of other G proteins, such as $G\alpha_q$, which is known to bind to human RIC8B in vitro (Klattenhoff et al., 2003).

Insertional mutagenesis by enhancer trapping

In this study, we isolated two phenotypic mutants out of 54 enhancer trap insertions. Although this frequency is not far superior to that with retroviral insertional mutagenesis in which one in 80 insertions caused embryonic lethality (Amsterdam et al., 1999), we think insertional mutagenesis by enhancer trapping should have the following merits. First, only a small number of F1 fish that show interesting GFP expression patterns need to be raised. Second, as heterozygous fish carrying same insertions can be identified in the F1 generation, it is not necessary to raise a large number of F2 fish, and, instead, homozygous phenotypes can be detected by analyzing F2 embryos. Third, as the place to be analyzed is illuminated by GFP, subtle morphological defects, such as fin phenotypes in the *tcf7* mutant, can be identified. Finally, as insertions are 'visible', carriers can be easily maintained without time-consuming genotyping. We demonstrated that our enhancer trap construct can be integrated within transcribed regions at a relatively high frequency. It is higher than that calculated for retroviral enhancer trap insertions, although it is not statistically different from that calculated for random integration. This finding opened a possibility that insertional mutagenesis could be performed more efficiently if an enhancer trap construct that can disrupt the function of target genes more efficiently was developed; for example, development of enhancer trap constructs carrying more elements to interfere with endogenous transcripts, such as a splice acceptor plus a polyA signal, etc. Studies along this line are in progress in our laboratory. In conclusion, our present study provided a basis for the development of efficient transposon-mediated insertional mutagenesis in a vertebrate.

We thank R. Dorsky for helpful discussion, and T. Uematsu, N. Mouri, S. Takeda, R. Mimura and M. Mizushina for fish room works. This work was supported by NIH R01 GM69382 and National BioResource Project, and by grants from the Ministry of Education, Culture, Sports, Science and Technology of Japan.

Supplementary material

Supplementary material for this article is available at http://dev.biologists.org/cgi/content/full/135/1/159/DC1

References

Abe, G., Ide, H. and Tamura, K. (2007). Function of FGF signaling in the developmental process of the median fin fold in zebrafish. *Dev. Biol.* **304**, 355-366.

Agarwal, P., Wylie, J. N., Galceran, J., Arkhitko, O., Li, C., Deng, C., Grosschedl, R. and Bruneau, B. G. (2003). Tbx5 is essential for forelimb bud initiation following patterning of the limb field in the mouse embryo. *Development* **130**, 623-633.

Akimenko, M. A., Ekker, M., Wegner, J., Lin, W. and Westerfield, M. (1994). Combinatorial expression of three zebrafish genes related to distal-less: part of a homeobox gene code for the head. *J. Neurosci.* **14**, 3475-3486.

Amsterdam, A. and Becker, T. S. (2005). Transgenes as screening tools to probe and manipulate the zebrafish genome. *Dev. Dyn.* **234**, 255-268.

Amsterdam, A., Burgess, S., Golling, G., Chen, W., Sun, Z., Townsend, K., Farrington, S., Haldi, M. and Hopkins, N. (1999). A large-scale insertional mutagenesis screen in zebrafish. *Genes Dev.* **13**, 2713-2724.

Amsterdam, A., Nissen, R. M., Sun, Z., Swindell, E. C., Farrington, S. and Hopkins, N. (2004). Identification of 315 genes essential for early zebrafish development. *Proc. Natl. Acad. Sci. USA* **101**, 12792-12797.

Balciunas, D., Davidson, A. E., Sivasubbu, S., Hermanson, S. B., Welle, Z. and Ekker, S. C. (2004). Enhancer trapping in zebrafish using the Sleeping Beauty transposon. *BMC Genomics* **5**, 62.

Barresi, M. J., Stickney, H. L. and Devoto, S. H. (2000). The zebrafish slow-muscle-omitted gene product is required for Hedgehog signal transduction and the development of slow muscle identity. *Development* **127**, 2189-2199.

Blackshear, P. J., Graves, J. P., Stumpo, D. J., Cobos, I., Rubenstein, J. L. and Zeldin, D. C. (2003). Graded phenotypic response to partial and complete deficiency of a brain-specific transcript variant of the winged helix transcription factor RFX4. *Development* **130**, 4539-4552.

Brown, S. A., Imbalzano, A. N. and Kingston, R. E. (1996). Activator-dependent regulation of transcriptional pausing on nucleosomal templates. *Genes Dev.* **10**, 1479-1490.

Driever, W., Solnica-Krezel, L., Schier, A. F., Neuhauss, S. C., Malicki, J., Stemple, D. L., Stainier, D. Y., Zwartkruis, F., Abdelilah, S., Rangini, Z. et al. (1996). A genetic screen for mutations affecting embryogenesis in zebrafish. *Development* **123**, 37-46.

Ellingsen, S., Laplante, M. A., Konig, M., Kikuta, H., Furmanek, T., Hoivik, E. A. and Becker, T. S. (2005). Large-scale enhancer detection in the zebrafish genome. *Development* **132**, 3799-3811.

Felsenstein, J. (1985). Confidence limits on phylogenies: an approach using the bootstrap. *Evolution* **39**, 783-791.

Fischer, S., Draper, B. W. and Neumann, C. J. (2003). The zebrafish fgf24 mutant identifies an additional level of Fgf signaling involved in vertebrate forelimb initiation. *Development* **130**, 3515-3524.

Gaiano, N., Amsterdam, A., Kawakami, K., Allende, M., Becker, T. and Hopkins, N. (1996). Insertional mutagenesis and rapid cloning of essential genes in zebrafish. *Nature* **383**, 829-832.

Galceran, J., Farinas, I., Depew, M. J., Clevers, H. and Grosschedl, R. (1999). Wnt3a–/–-like phenotype and limb deficiency in Lef1(–/–)Tcf1(–/–) mice. *Genes Dev.* **13**, 709-717.

Haffter, P., Granato, M., Brand, M., Mullins, M. C., Hammerschmidt, M., Kane, D. A., Odenthal, J., van Eeden, F. J., Jiang, Y. J., Heisenberg, C. P. et al. (1996). The identification of genes with unique and essential functions in the development of the zebrafish, Danio rerio. *Development* **123**, 1-36.

Halloran, M. C., Sato-Maeda, M., Warren, J. T., Su, F., Lele, Z., Krone, P. H., Kuwada, J. Y. and Shoji, W. (2000). Laser-induced gene expression in specific cells of transgenic zebrafish. *Development* **127**, 1953-1960.

Kawakami, K. (2004). Transgenesis and gene trap methods in zebrafish by using the Tol2 transposable element. *Methods Cell Biol.* **77**, 201-222.

Kawakami, K. (2005). Transposon tools and methods in zebrafish. *Dev. Dyn.* **234**, 244-254.

Kawakami, K. and Shima, A. (1999). Identification of the Tol2 transposase of the medaka fish Oryzias latipes that catalyzes excision of a nonautonomous Tol2 element in zebrafish Danio rerio. *Gene* **240**, 239-244.

Kawakami, K., Koga, A., Hori, H. and Shima, A. (1998). Excision of the Tol2 transposable element of the medaka fish, Oryzias latipes, in zebrafish, Danio rerio. *Gene* **225**, 17-22.

Kawakami, K., Shima, A. and Kawakami, N. (2000). Identification of a functional transposase of the Tol2 element, an Ac-like element from the Japanese medaka fish, and its transposition in the zebrafish germ lineage. *Proc. Natl. Acad. Sci. USA* **97**, 11403-11408.

Kawakami, Y., Capdevila, J., Buscher, D., Itoh, T., Rodriguez Esteban, C. and Izpisua Belmonte, J. C. (2001). WNT signals control FGF-dependent limb initiation and AER induction in the chick embryo. *Cell* **104**, 891-900.

Kawakami, K., Takeda, H., Kawakami, N., Kobayashi, M., Matsuda, N. and Mishina, M. (2004). A transposon-mediated gene trap approach identifies developmentally regulated genes in zebrafish. *Dev. Cell* **7**, 133-144.

Kengaku, M., Capdevila, J., Rodriguez-Esteban, C., De La Pena, J., Johnson, R. L., Belmonte, J. C. and Tabin, C. J. (1998). Distinct WNT pathways regulating AER formation and dorsoventral polarity in the chick limb bud. *Science* **280**, 1274-1277.

Kent, W. J. (2002). BLAT-the BLAST-like alignment tool. *Genome Res.* **12**, 656-664.
Kikuta, H., Laplante, M., Navratilova, P., Komisarczuk, A. Z., Engstrom, P. G., Fredman, D., Akalin, A., Caccamo, M., Sealy, I., Howe, K. et al. (2007). Genomic regulatory blocks encompass multiple neighboring genes and maintain conserved synteny in vertebrates. *Genome Res.* **17**, 545-555.
Klattenhoff, C., Montecino, M., Soto, X., Guzman, L., Romo, X., Garcia, M. A., Mellstrom, B., Naranjo, J. R., Hinrichs, M. V. and Olate, J. (2003). Human brain synembryn interacts with Gsalpha and Gqalpha and is translocated to the plasma membrane in response to isoproterenol and carbachol. *J. Cell. Physiol.* **195**, 151-157.
Kotani, T., Nagayoshi, S., Urasaki, A. and Kawakami, K. (2006). Transposon-mediated gene trapping in zebrafish. *Methods* **39**, 199-206.
Logan, D. W., Burn, S. F. and Jackson, I. J. (2006). Regulation of pigmentation in zebrafish melanophores. *Pigment Cell Res.* **19**, 206-213.
Miller, K. G., Emerson, M. D., McManus, J. R. and Rand, J. B. (2000). RIC-8 (Synembryn): a novel conserved protein that is required for G (q)alpha signaling in the C. elegans nervous system. *Neuron* **27**, 289-299.
Mlodzik, M. and Hiromi, Y. (1992). Enhancer trap method in *Drosophila*: its application to neurobiology. In *Methods in Neurosciences*. Vol. 9 (ed. P. M. Conn), pp. 397-414. San Diego: Academic Press.
Ng, J. K., Kawakami, Y., Buscher, D., Raya, A., Itoh, T., Koth, C. M., Rodriguez Esteban, C., Rodriguez-Leon, J., Garrity, D. M., Fishman, M. C. et al. (2002). The limb identity gene Tbx5 promotes limb initiation by interacting with Wnt2b and Fgf10. *Development* **129**, 5161-5170.
Norton, W. H., Ledin, J., Grandel, H. and Neumann, C. J. (2005). HSPG synthesis by zebrafish Ext2 and Extl3 is required for Fgf10 signalling during limb development. *Development* **132**, 4963-4973.
Parinov, S., Kondrichin, I., Korzh, V. and Emelyanov, A. (2004). Tol2 transposon-mediated enhancer trap to identify developmentally regulated zebrafish genes in vivo. *Dev. Dyn.* **231**, 449-459.
Reifers, F., Bohli, H., Walsh, E. C., Crossley, P. H., Stainier, D. Y. and Brand, M. (1998). Fgf8 is mutated in zebrafish acerebellar (ace) mutants and is required for maintenance of midbrain-hindbrain boundary development and somitogenesis. *Development* **125**, 2381-2395.
Rougvie, A. E. and Lis, J. T. (1988). The RNA polymerase II molecule at the 5′ end of the uninduced hsp70 gene of D. melanogaster is transcriptionally engaged. *Cell* **54**, 795-804.
Rzhetsky, A. and Nei, M. (1992). Statistical properties of the ordinary least-squares, generalized least-squares, and minimum-evolution methods of phylogenetic inference. *J. Mol. Evol.* **35**, 367-375.
Saitou, N. and Nei, M. (1987). The neighbor-joining method: a new method for reconstructing phylogenetic trees. *Mol. Biol. Evol.* **4**, 406-425.
Schade, M. A., Reynolds, N. K., Dollins, C. M. and Miller, K. G. (2005). Mutations that rescue the paralysis of Caenorhabditis elegans ric-8 (synembryn) mutants activate the G alpha (s) pathway and define a third major branch of the synaptic signaling network. *Genetics* **169**, 631-649.
Scott, E. K., Mason, L., Arrenberg, A. B., Ziv, L., Gosse, N. J., Xiao, T., Chi, N. C., Asakawa, K., Kawakami, K. and Baier, H. (2007). Targeting neural circuitry in zebrafish using GAL4 enhancer trapping. *Nat. Methods* **4**, 323-326.
Seamon, K. B., Padgett, W. and Daly, J. W. (1981). Forskolin: unique diterpene activator of adenylate cyclase in membranes and in intact cells. *Proc. Natl. Acad. Sci. USA* **78**, 3363-3367.
Tall, G. G., Krumins, A. M. and Gilman, A. G. (2003). Mammalian Ric-8A (synembryn) is a heterotrimeric Galpha protein guanine nucleotide exchange factor. *J. Biol. Chem.* **278**, 8356-8362.
Thompson, J. D., Higgins, D. G. and Gibson, T. J. (1994). CLUSTAL W: improving the sensitivity of progressive multiple sequence alignment through sequence weighting, position-specific gap penalties and weight matrix choice. *Nucleic Acids Res.* **22**, 4673-4680.
Uemura, O., Okada, Y., Ando, H., Guedj, M., Higashijima, S., Shimazaki, T., Chino, N., Okano, H. and Okamoto, H. (2005). Comparative functional genomics revealed conservation and diversification of three enhancers of the isl1 gene for motor and sensory neuron-specific expression. *Dev. Biol.* **278**, 587-606.
Urasaki, A., Morvan, G. and Kawakami, K. (2006). Functional dissection of the Tol2 transposable element identified the minimal cis-sequence and a highly repetitive sequence in the subterminal region essential for transposition. *Genetics* **174**, 639-649.
Veien, E. S., Grierson, M. J., Saund, R. S. and Dorsky, R. I. (2005). Expression pattern of zebrafish tcf7 suggests unexplored domains of Wnt/beta-catenin activity. *Dev. Dyn.* **233**, 233-239.

Table S1. Expression patterns and integration sites in enhancer trap lines

Insertion	Accession	GFP pattern	Stage	Nearest gene	Position	Expression	Homo
HG2A	AB353972	Myotome	24 hpf	AB247645 (chot1)*	intron	myotome*	viable
HG3A	AB353973	Skin	24 hpf	AB303423 (cyp2e2)*	intron	skin*	viable
HG6A	AB353974	Myotome	24 hpf	AB303424 (ide)*	intron	myotome*	viable
HG6B	AB353975	Head, myotome	24 hpf	AB247646 (soxlz)*	intron	myotome*	viable
HG6C	AB353976	Notochord	24 hpf	AB303425 (uros)*	intron	ventral mesoderm*	viable
HG6D	AB353977	Myotome	24 hpf	AB303426 (asb1)*	intron	whole body (weak)*	viable
HG9B	AB353978	Cells on the skin	24 hpf	ENSDARG00000063017 (TTLL4 homolog)	exon	whole body (weak)*	viable
HG9C	AB353979	Cranial ganglia	24 hpf	NA			viable
HG10A	AB353980	Forebrain, myotome	24 hpf	zgc:76938 (fancl)	exon	NA	viable
HG10B	AB353981	Cells on the skin	24 hpf	AB303427 (ripk2)*	intron	whole body (weak)*	viable
HG10C	AB353982	Whole body	24 hpf	NA			viable
HG21A	AB353983	Myotome	24 hpf	AB247647 (lmo7)*	intron	myotome*	viable
HG21B	AB353987	Otic vesicle, myotome	24 hpf	AB247648 (novel gene)*	intron	otic vesicle*	viable
HG21C	AB353984	Fin folds	24 hpf	AB303428 (tcf7)*	exon	fin folds*	fin defects
HG21E	AB353985	Forebrain, eye	24 hpf	zgc:92692 (crystallin homolog)	15 kb downstream	NA	viable
HG21K	AB353986	Spinal cord	24 hpf	ENSDARG00000062396 (novel gene)	7.5 kb downstream	NA	viable
HGn6A	AB353988	Whole body	26 hpf	NA			viable
HGn8E	AB353989	Heart	24 hpf	ENSDARG00000054207 (sialyltransferase homolog)	intron	NA	viable
HGn8H	AB353990	CNS	24 hpf	AB354736 (synbl)	intron	whole body*	lethal
HGn12B	AB353991	Otic vesicle	25 hpf	zgc:65749 (unknown)	2 kb upstream	NA	viable
HGn12C	AB353992	Pretectum	30 hpf	NA			viable
HGn12F	AB353993	Brain, lens	day 3	NA			ND
HGn12H	AB353994	Brain	day 5	ENSDARG00000027887 (zfyve21)	47 kb downstream	whole body, brain	ND
HGn12J	AB353995	Floor plate	24 hpf	zgc:66419 (hook homolog)	45 kb upstream	NA	viable
HGn14C	AB353996	Myotome and lens	36 hpf	NA			viable
HGn15A	AB353997	Notochord	24 hpf	ENSDARG00000005333 (tln1)	intron	notochord	viable
HGn15B	AB353998	Whole body	24 hpf	ENSDARG00000061750 (sphingomyelin synthase homolog)	7.7 kb upstream	NA	ND
HGn16A	AB353999	Forebrain, hindbrain, myotome	24 hpf	NA			viable
HGn20A	AB354000	Forebrain, MHB	36 hpf	zgc:158431 (unknown)	56 kb upstream	NA	ND
HGn20B	AB354001	Hindbrain	36 hpf	NA			ND
HGn20C	AB354002	Midbrain	24 hpf	ENSDARG00000015243 (novel gene)	21 kb upstream	NA	ND
HGn20D	AB354003	Tectum	25 hpf	zgc:55390 (ampd3)	112 kb upstream	blood, epidermis	ND
HGn20E	AB354004	Pectoral fin	48 hpf	zgc:136669 (egfl7)	intron	NA	ND
HGn21A	AB354005	Notochord	24 hpf	ENSDARG00000007356 (fgf20a)	1.7 kb upstream	NA	viable
HGn22A	AB354006	Eye, myotome	26 hpf	zgc:86646 (rcn3)	3.8 kb upstream	head, notochord	viable
HGn23A	AB354007	Nose, lens	day 3	NA			ND
HGn25A	AB354008	Neural tube	24 hpf	ENSDARG00000071496 (zic6)*	57 kb downstream	NA	viable
HGn25B	AB354009	Otic vesicle	26 hpf	ENSDARG00000032868 (PDE homolog)	46 kb upstream	—	viable
HGn25C	AB354010	Forebrain	24 hpf	ENSDARG00000039495 (unknown)	210 kb upstream	NA	viable
HGn25D	AB354011	Law, lens, heart	day 3	NA			ND
HGn26A	AB354012	Myotome, skin	34 hpf	NA			viable
HGn26B	AB354013	Eye, forebrain, tectum	25 hpf	NA			viable
HGn28A	AB354014	Otic vesicle, arches, skin	24 hpf	ENSDARG00000016526 (gata3)	26 kb downstream	otic vesicle, arches, etc	viable
HGn30A	AB354015	Hatching gland	24 hpf	NA			viable
HGn31A	AB354016	Forebrain, hindbrain, spinal cord	24 hpf	NA			ND
HGn31B	AB354017	Cranial ganglis, spinal cord	26 hpf	ENSDARG00000023288 (novel gene)	103 kb downstream	NA	ND

HGn32A	AB354018	Hindbrain	33 hpf	NA			viable
HGn32B	AB354019	Midbrain	26 hpf	ENSDARG00000039412 (dmrta2)*	36 kb downstream	NA	viable
HGn34A	AB354020	Myotome, fin folds	24 hpf	ENSDARG00000003217 (unknown)	17 kb downstream	NA	ND
HGn34B	AB354021	CNS, eye	24 hpf	ENSDARG00000006837 (mycn)	17 kb downstream	brain	viable
HGn36A	AB354022	Neurons	36 hpf	ENSDARG00000021733 (unknown)	5.1 kb downstream	NA	viable
HGn39B	AB354023	Heart, myotome	24 hpf	zgc:136821 (ahsa1)	intron	myotome	viable
HGn39C	AB354024	Whole body	24 hpf	NA			viable
HGn39D	AB354025	Lateral line, lens	day 5	ENSDARG00000063251 (unknown)	0.6 kb upstream	NA	viable
HGn42A	AB354026	Eye	24 hpf	ENSDARG00000054327 (novel gene)	20 kb upstream	NA	viable
HGn42D	AB354027	Myotome	day 5	ENSDARG00000060236 (dok7)	intron	NA	viable
HGn43A	AB354028	Forebrain	26 hpf	ENSDARG00000061191 (novel gene)	intron	NA	viable
HGn44B	AB354029	Hindbrain, spinal cord	31 hpf	ENSDARG00000005783 (ncan)	intron	NA	ND
HGn44E	AB354030	Myotome	31 hpf	NA			ND
HGn46C	AB354031	Telencephalon	25 hpf	zgc:56483 (vrk2)	0.5 kb upstream	NA	viable
HGn46E	AB354032	Notochord	30 hpf	NA			viable
HGn46F	AB354033	Myotome, yolk	30 hpf	ENSDARG00000057057 (novel gene)	61 kb upstream	NA	viable
HGn50A	AB354034	Forebrain	26 hpf	NA			ND
HGn50B	AB354035	Epiphysis, nose	25 hpf	ENSDARG00000053026 (kinesin homolog)	intron	NA	viable
HGn50D	AB354037	Yolk	24 hpf	NA			viable
HGn50E	AB354036	Brain, lens	day 5	NA			viable
HGn50G	AB354038	Myotome, fin folds	36 hpf	ENSDARG00000062126 (unknown)	12 kb upstream	NA	viable
HGn53D	AB354039	Fin folds	24 hpf	ENSDARG00000011512 (novel gene)	intron	NA	viable
HGn54A	AB354040	Hatching gland	34 hpf	ENSDARG00000057975 (PLC)	9 kb downstream	NA	ND
HGn54B	AB354041	Cells on the skin	24 hpf	ENSDARG00000040059 (gbp)	19 kb upstream	whole body, CNS	ND
HGn62A	AB354042	Skin	33 hpf	NA			viable
HGn62B	AB354043	Hatching gland	25 hpf	zgc:112012 (semaphorin homolog)	172 kb upstream	rhombomres, etc	viable
HGn63B	AB354044	CNS	27 hpf	ENSDARG00000061139 (G-protein coupled receptor homolog)	21 kb downstream	NA	ND

NA in the nearest gene column: not applicable as the cloned sequence was not mapped on the genome.
NA in the pattern column: expression patterns revealed by whole-mount in situ pattern are not available.
ND in the homo column: the phenotypes of homozygous embryos have not been determined.
*Cloning of cDNA and in situ hybridization were performed in this study.